Cancer Chemother Pharmacol (2009) 63:1049–1063
DOI 10.1007/s00280-008-0827-2

ORIGINAL ARTICLE

Mechanistic population pharmacokinetics of total and unbound paclitaxel for a new nanodroplet formulation versus Taxol in cancer patients

Jürgen B. Bulitta · Ping Zhao · Robert D. Arnold · Dean R. Kessler · Richard Daifuku · James Pratt · Gabriel Luciano · Axel-R Hanauske · Hans Gelderblom · Ahmad Awada · William J. Jusko

Received: 1 April 2008 / Accepted: 17 August 2008 / Published online: 13 September 2008

Abstract
Purpose Our objectives were (1) to compare the disposition and in vivo release of paclitaxel between a tocopherol-based Cremophor-free formulation (Tocosol Paclitaxel®) and Cremophor® EL-formulated paclitaxel (Taxol®) in human subjects, and (2) to develop a mechanistic model for unbound and total paclitaxel pharmacokinetics.
Methods A total of 35 patients (average ± SD age: 59 ±13 years) with advanced non-hematological malignancies were studied in a randomized two-way crossover trial. Patients received 175 mg/m^2 paclitaxel as 15 min (Tocosol Paclitaxel) or 3 h (Taxol) intravenous infusion in each study period. Paclitaxel concentrations were determined by LC–MS/MS in plasma ultrafiltrate and whole blood. NONMEM VI was used for population pharmacokinetics.
Results A linear disposition model with three compartments for unbound paclitaxel and a one-compartment model for Cremophor were applied. Total clearance of unbound paclitaxel was 845 L/h (variability: 25% CV). The prolonged release with Tocosol Paclitaxel was explained by the limited solubility of unbound paclitaxel of 405 ng/mL (estimated) in plasma. The 15 min Tocosol Paclitaxel infusion yielded a mean time to 90% cumulative input of 1.14 ± 0.16 h. Tocosol Paclitaxel was estimated to release 9.8% of the dose directly into the deep peripheral compartment. The model accounted for the presence of drug-containing nanodroplets in blood.
Conclusions Population pharmacokinetic analysis indicated linear disposition and a potentially higher bioavailability of unbound paclitaxel following Tocosol Paclitaxel administration due to direct release at the target site. The prolonged release of Tocosol Paclitaxel supports 15 min paclitaxel infusions. This mechanistic model may be important for development of prolonged release formulations that distribute in and from the systemic circulation.

Keywords Paclitaxel · Ultrafiltration · Non-hematological malignancies · Mechanistic modeling · Population pharmacokinetics · NONMEM · Solubility limited disposition model

This modeling analysis was in part presented as a poster at the American Conference on Pharmacometrics (ACoP) 2008, Tucson, AZ. The data and non-compartmental pharmacokinetic analysis of this study were in part presented at the 2005 Annual Meeting of the American Society of Clinical Oncology (Abstract no. 2045), Orlando, FL.

J. B. Bulitta · R. D. Arnold · W. J. Jusko (✉)
Department of Pharmaceutical Sciences, School of Pharmacy and Pharmaceutical Sciences, University at Buffalo, State University of New York, Hochstetter Hall, Room 565, Buffalo, NY 14260-1200, USA
e-mail: wjjusko@buffalo.edu

P. Zhao · D. R. Kessler · R. Daifuku · J. Pratt · G. Luciano
Sonus Pharmaceuticals, Inc., Bothell, WA 98021, USA

A.-R. Hanauske
Department of Medical Oncology, St. Georg Hospital, Lohmühlenstr. 5, 20099 Hamburg, Germany

H. Gelderblom
Department of Clinical Oncology, Leiden University Medical Center, Leiden, The Netherlands

A. Awada
Institut Jules Bordet, Rue Heger-Bordet 1, 1000 Brussels, Belgium

Present Address:
R. D. Arnold
Department of Pharmaceutical and Biomedical Sciences, University of Georgia, Athens, GA 30602-2352, USA

Introduction

Paclitaxel is a clinically important antitumor agent with activity against a wide array of cancers [27]. Due to the low aqueous solubility of paclitaxel, the most commonly used paclitaxel formulation (Taxol) contains Cremophor EL (polyoxyethylated castor oil) and ethanol (1:1, w/w) to solubilize paclitaxel. Cremophor is associated with hypersensitivity reactions due to complement activation [8, 42, 44]. Other studies [2, 47] suggest that Cremophor is involved in peripheral sensory neuropathy. Cremophor affects the pharmacokinetics (PK) of paclitaxel by entrapment of paclitaxel inside Cremophor micelles which are major "binding" sites for paclitaxel in vitro [34], in animals [32, 33], and in humans [14, 16]. Other binding sites for paclitaxel are albumin and α_1-acid glycoprotein [22], red blood cells [34], and platelets [46].

Hepatic metabolism and biliary excretion are the primary routes of paclitaxel elimination [23, 43]. Non-linear PK of total paclitaxel in blood was associated with saturable elimination [30], saturable distribution [19], and binding to Cremophor [14, 16, 34, 40–42]. This non-linearity seems to be less pronounced if the duration of infusion is longer than 6 h [4, 45]. More recent studies measured unbound paclitaxel concentrations and found linear disposition of unbound paclitaxel [9, 15, 16].

For PK comparison of a Cremophor-containing formulation and a Cremophor-free formulation, it is important to measure both unbound and total paclitaxel concentrations. We studied a new tocopherol-based, Cremophor-free paclitaxel formulation (Tocosol Paclitaxel) in comparison to Taxol. Two key advantages of Tocosol Paclitaxel are the absence of Cremophor-related toxicity and the ability to administer Tocosol Paclitaxel as a 15-min infusion (compared to 3 or 24 h infusion for Taxol). This rapid infusion is possible, since paclitaxel is contained within nanodroplets that release paclitaxel over time. Tocosol Paclitaxel nanodroplets have a diameter of 40–80 nm [5, 6], are stable and neutrally charged. These nanodroplets have the potential to distribute into tumor tissue and release a fraction of the paclitaxel dose directly at the target site, since pore sizes of many tumor tissues are larger than the tight endothelial junctions of normal tissue vasculature [28]. Direct release of drug from drug-containing nanodroplets that distribute to the target site would result in a greater unbound area under the concentration time curve (AUC) at the target site compared to the AUC in plasma. This may reduce the toxicity of paclitaxel at sites not accessible to Tocosol Paclitaxel nanodroplets.

Population PK methodology was used to consider direct paclitaxel release to a peripheral compartment. Assessing the presence of paclitaxel containing nanodroplets in blood samples requires a modeling approach, as unreleased paclitaxel in nanodroplets contributes to the observed concentrations. Additionally, it seems likely that some drug may be released from nanodroplets during the centrifugation of blood samples. The possible contribution of these processes was examined for the data collected using a modeling approach.

Our first objective was to compare the PK of paclitaxel in plasma ultrafiltrate and in whole blood between Tocosol Paclitaxel and Taxol by population modeling. Secondly, we sought to characterize the rate and extent of paclitaxel release from the Tocosol Paclitaxel formulation accounting for the presence of drug-containing nanodroplets in blood. We were especially interested in quantifying the amount of paclitaxel that was released directly into a peripheral compartment, since direct release at the target site would increase the availability at the site of action.

Materials and methods

Study design and patients

The study was a randomized, two-period, open label, multicenter (6 clinical sites), crossover study in 36 adult patients. The inclusion criteria were: (1) histological diagnosis of advanced non-hematological malignancy for which there was no curative therapy and for which treatment with a single agent taxane was appropriate according to the opinion of the treating physician, (2) no more than two prior cytotoxic chemotherapy regimens for metastatic disease (not including adjuvant or neoadjuvant chemotherapy for primary disease), (3) adequate hematological, renal and liver function, (4) peripheral neuropathy grade 0–1 per NCI-CTC, (5) Eastern Cooperative Oncology Group (ECOG) [26] performance status of 0–2, (6) absolute neutrophil count above 2,000 cells/mm^3, and (7) platelet count above 100,000/mm^3. The study was approved by all relevant Ethics Committees and Institutional Review Boards and was conducted following the revised version of the Declaration of Helsinki. Written informed consent forms were signed by each patient prior to inclusion in the study.

Drug administration

Each patient received a dose of 175 mg/m^2 paclitaxel (about 300 mg for a patient with 1.73 m^2 body surface area, BSA) as Tocosol Paclitaxel in study period I followed by the same dose of Taxol in study period II or vice versa. The washout period was 3 weeks. Paclitaxel was given as a constant rate infusion over approximately 15 min for Tocosol Paclitaxel and 3 h for Taxol.

Paclitaxel was infused intravenously with a controlled-rate infusion pump. The infusion rate was about 2 mL/min for Tocosol Paclitaxel. A paclitaxel concentration of 10 mg/mL yielded a total infused volume of about 30 mL for a patient with 1.73 m^2 BSA. Syringes, infusion pumps and intravenous (IV) tubing sets were provided by Sonus Pharmaceuticals. Patients were monitored closely and asked about any symptoms or adverse effects during the 15 min infusion. In case any symptoms occurred, the infusion was interrupted and resumed within 30 min, if resuming was deemed safe by the responsible physician. The exact infusion times and volumes were recorded and used for PK modeling. According to the clinical protocol, all patients were treated with a fixed regimen of antihistamines (H_1 and H_2 blockade) and glucocorticoids 30–60 min prior to drug administration in study phases I and II. This included diphenhydramine 50 mg IV, cetirizine 10 mg PO, or clemastine 2 mg IV as well as ranitidine 50 mg IV and dexamethasone 20 mg IV. Granisetron 10 μg/kg IV at 30–60 min before dosing was an optional premedication.

The appropriate dose of Taxol was prepared as an IV admixture in 0.9% saline or 5% dextrose in water to yield a final concentration of approximately 1 mg of paclitaxel per mL of dosing solution (total volume: about 300 mL for a patient with 1.73 m^2 to be infused within 3 h). Taxol was infused at a constant rate of about 1.67 mL/min via a standard infusion set with a 0.22 μm in-line filter. Only glass, polypropylene and polyolefin containers were used, as Taxol solutions have been shown to extract DEHP plasticizer from PVC containers according to the Taxol package insert. Patients were carefully monitored and asked about symptoms and adverse effects during the infusion.

Blood sampling

In each study period, 4 mL of blood was taken at 18 specified time points. For Tocosol Paclitaxel, samples were taken immediately before start of the infusion, at 5, 10, and 15 min post-start and 5, 15, 30, and 60 min after end of Tocosol Paclitaxel infusion as well as at 2, 3, 5, 8, 14, 24, 48, 72, 96, and 120 h. For Taxol, blood sampling times were immediately before start of infusion and 1, 2, and 3 h post start, 5, 15, 30, and 45 min post end of infusion as well as at 2, 4, 6, 9, 14, 24, 48, 72, 96, and 120 h. If the infusion was interrupted, additional blood samples were taken immediately after such interruption and immediately before resuming infusion.

Blood was collected into EDTA tubes and samples were kept in a temperature controlled water bath at 37°C until processing. Two aliquots each of 0.5 mL whole blood were prepared from each blood sample. The remaining 3 mL blood was centrifuged at 10,000*g* for 15 min at 37°C to prepare two plasma aliquots from each sample. Blood and plasma samples were frozen immediately and stored at −20°C prior to analysis.

Drug analysis

Preparation of plasma ultrafiltrate specimens from patient blood samples began within 20 min of drawing each blood sample and was completed without delay. Whole blood and plasma ultrafiltrate samples were frozen at the site, and shipped frozen to the analytical lab, where the samples were extracted by methyl tert-butyl ether and analyzed for paclitaxel concentrations using validated methods. The assay was validated from 0.1 to 50 ng/mL for plasma ultrafiltrate using an extraction volume of 80 μL and from 5 to 5,000 ng/mL for whole blood using an extraction volume of 100 μL. The method used liquid chromatography coupled to tandem mass spectrometry (LC–MS/MS), which included a Perkin Elmer Series 200 Micro LC pump (Perkin Elmer, Waltham, MA), a CTC-PAL auto sampler (LEAP Technologies, LLC, Carrboro, NC), and an API 3000 or 4000 mass spectrometer with a TurboIon Spray® source (Applied Biosystems, Foster City, CA). Chromatographic separation was performed on a Phenomenex Curosil-PFP column (3 μm, 50 × 2 mm, Phenemonex Inc, Torrance, CA) at a flow rate of 0.5 mL/min using a linear gradient elution of water and acetonitrile (0–2.0 min: 30–70% acetonitrile; 2.0–2.5 min: 70–90% acetonitrile; 2.5–2.7 min: 90% acetonitrile; and 2.7–2.9 min: 90–30% acetonitrile). Detection of analytes was by positive-ion mode using multiple reaction monitoring scan mode, with ion transitions m/z 854 → 286 for paclitaxel and m/z 860 → 292 for $^{13}C_6$-paclitaxel (internal standard). The lower limit of quantification was 0.1 ng/mL in plasma ultrafiltrate and 5 ng/mL in whole blood.

Correlation coefficients for regression of calibration curves were at least 0.984 for plasma ultrafiltrate and at least 0.988 for whole blood. For back-calculated standard concentrations, mean accuracy (% bias) ranged from −1.7 to 2.2% for ultrafiltrate and from −3.4 to 4.8% for whole blood; the precision (% coefficient of variation, %CV), ranged from 5.4 to 8.4% for ultrafiltrate and from 6.1 to 7.8% for whole blood. For quality control samples, the accuracy ranged from −20.3 to 9.8% for ultrafiltrate and from −9.9 to 8.5% for whole blood; the precision ranged from 8.0 to 15.9% for ultrafiltrate and from 8.4 to 14.3% for whole blood.

Laboratory testing

A complete blood count, chemistry panel, prothrombin time, partial thromboplastin time and pregnancy test (if applicable) were performed within 1 week before study drug administration in study period 1 and within 1 day before administration in study period 2. Additionally, a complete blood count including absolute neutrophil count

was performed on days 1, 4, 7, 10, 13, and 16 during the 21 days after each dose.

Population PK analysis

Drug input for Tocosol Paclitaxel

The duration of infusion documented by the clinical site for each subject/dose was used for PK modeling for both formulations. If the infusion was interrupted, the exact infusion times were used. Drug input for Tocosol Paclitaxel was described as time-delimited zero-order input process (rate: R_{Input}, relative extent of bioavailability compared to Taxol: F_{Tocosol}) into the "nanodroplet compartment" (A_{Nano}). The following equation and initial condition described the input into and saturable release from A_{Nano} for the model shown in Fig. 1:

$$\frac{dA_{\text{Nano}}}{dt} = F_{\text{Tocosol}} \cdot R_{\text{Input}} - \frac{V_{\max} \cdot A_{\text{Nano}}}{AN_{50} + A_{\text{Nano}}}. \quad (1)$$

The initial condition of this equation is zero. The $V_{\max}$ is the maximum release rate and AN_{50} is the amount of drug in nanodroplet compartment that results in a release rate of 50% of $V_{\max}$. A mechanistic derivation of this equation based on solubility-limited transfer through an unstirred water layer is shown in the Appendix. In brief, $V_{\max}$ is determined by the product of the volume of the putative unstirred water-layer around Tocosol nanodroplets (V_{layer}), the paclitaxel solubility (C_{Sol}), and the rate constant of loss from this layer (ka_2). The AN_{50} is $V_{\max}$ divided by the rate constant of release into the unstirred water-layer (ka_1). In addition to drug release from nanodroplets into the central compartment, we considered models with simultaneous partial drug release into the peripheral compartments.

Disposition models for Tocosol Paclitaxel

Models with one, two, or three disposition compartments for paclitaxel in combination with (1) first-order, mixed-order, or parallel first-order and mixed-order elimination from the central compartment, and (2) first-order or mixed-order distribution to the shallow peripheral compartment were considered. The final model for Tocosol Paclitaxel had the following additional equations for unbound paclitaxel:

$$\frac{dA1}{dt} = (1 - Fr3) \cdot \frac{V_{\max} \cdot A_{\text{Nano}}}{AN_{50} + A_{\text{Nano}}} - (CL + CLd_2 + CLd_3) \cdot C1 + CLd_2 \cdot C2 + CLd_3 \cdot C3 \quad (2)$$

$$\frac{dA2}{dt} = CLd_2 \cdot (C1 - C2) \quad (3)$$

$$\frac{dA3}{dt} = Fr3 \cdot \frac{V_{\max} \cdot A_{\text{Nano}}}{AN_{50} + A_{\text{Nano}}} + CLd_3 \cdot (C1 - C3). \quad (4)$$

Initial conditions for these differential equations were zero (parameters are explained in Table 1 and shown in Fig. 1). The A1 is the amount in the central, A2 in the shallow peripheral, and A3 in the deep peripheral compartment (DPC). Unbound concentrations in these compartments (C1, C2, and C3) are the amounts divided by the respective volume terms. The fraction of paclitaxel

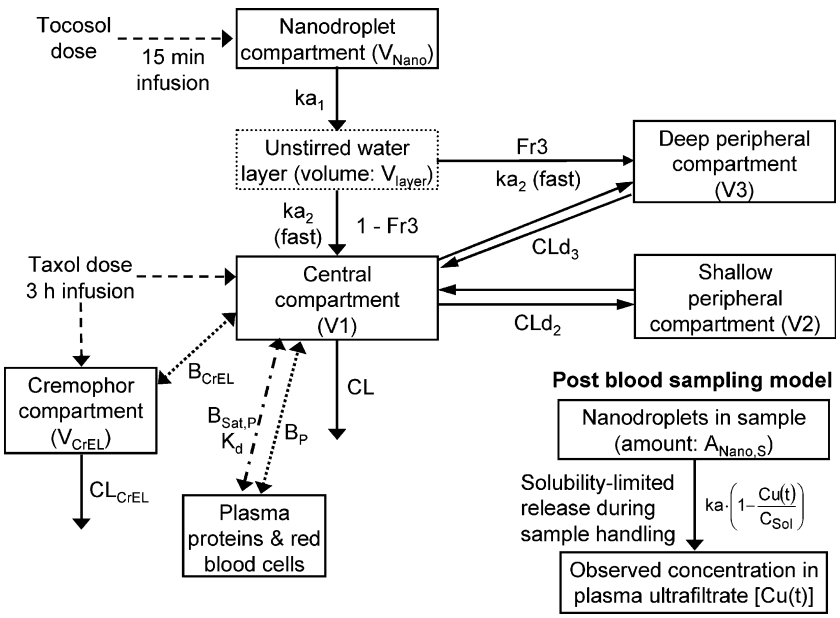

Fig. 1 Structural model for the release and disposition of paclitaxel, disposition of Cremophor, and nanodroplets as well as structural model for the release of paclitaxel from nanodroplets after the blood draw. *Symbols* are defined in Table 1 (see Appendix for details on first-order rate constants ka_1 and ka_2)

Table 1 Population pharmacokinetic parameter estimates and confidence intervals (CI)

Parameter	Symbol	Unit	Estimate (90% CI)	Variability (90% CI)[a]	ΔObj[d]
Disposition of paclitaxel					
Total clearance[b]	CL	L/h	845 (783–910)	25% (15–37%)	
Volume of central compartment[b]	V1	L	610 (430–718)	27% (0.3–40%)	
Volume of shallow peripheral compartment[b]	V2	L	1480 (1260–1710)	19% (3.8–27%)	
Volume of deep peripheral compartment[b]	V3	L	6830 (6080–7561)	24% (16–29%)	
Intercompartmental clearance to V2[b]	CLd_2	L/h	724 (631–918)	23% (0.2–33%)	
Intercompartmental clearance to V3[b]	CLd_3	L/h	317 (274–371)	23% (14–32%)	
Release from Tocosol Paclitaxel nanodroplets					
Relative extent of bioavailability for Tocosol Paclitaxel	$F_{Tocosol}$		0.940 (0.882–0.997)	(F_{Taxol} fixed to 1)	9.9[d]
Fraction of dose directly entering the deep peripheral compartment from nanodroplets	Fr3		0.098 (0.0443–0.153)		32
Maximum rate of release from nanodroplets	V_{max}	mg/h	356 (301–424)		
Amount of drug in nanodroplets for that the release rate is half-maximal	AN_{50}	mg	50.0 (27.7–78.8)	47% (34–64%)	233[d]
Solubility of unbound paclitaxel in plasma	C_{Sol}	ng/mL	405 (368–452)		155[d]
Volume of distribution of nanodroplets[b]	V_{Nano}	L	6.66 (6.03–7.35)	21% (16–24%)	29[d]
Half-life of release during sample handling if no saturation[e]	$t_{1/2}$(ka)	min	26.8[e] (19.8–36.2)	84% (56–120%)	936[d]
Disposition of Cremophor					
Total clearance of Cremophor[b]	CL_{CrEL}	L/h	0.583 (0.257–0.970)	203% (96–405%)	491
Volume of distribution of Cremophor[b]	V_{CrEL}	L	6.01 (fixed)		
Paclitaxel binding					
Linear binding to plasma proteins and red blood cells	B_P		21.0 (19.0–22.6)	13% (4.1–17%)	51
Maximum binding capacity divided by K_d	$B_{Sat,P}/K_d$		8.01 (3.72–13.0)	103% (48–200%)	51
Dissociation constant	K_d	ng/mL	4.38 (3.02–6.99)		
Linear binding of paclitaxel to Cremophor[c]	B_{CrEL}	L/g	6.61 (5.65–7.93)		491
Unbound concentration					
Proportional error		%	30.2 (27.0–32.9)		
Additive error		ng/mL	0.110 (0.0802–0.143)		
Total concentration					
Proportional error		%	17.3 (15.6–18.7)		
Additive error		ng/mL	2.25 (1.73–2.79)		

[a] Estimates are apparent coefficients of variation for the between-subject variability

[b] Per 1.73 m^2 body surface area

[c] Cremophor dose was 0.527 g purified Cremophor EL per 6 mg paclitaxel according to the Taxol package insert

[d] Increase in objective function after estimation of the simplified model, if the parameter mean was fixed to zero (exceptions: $F_{Tocosol}$ fixed to 1.0, V_{Nano} fixed to 5 L representing plasma volume, ka fixed to 0/h, and C_{Sol} and AN_{50} fixed to very large values). The final model was used as reference. An increase in the objective function by 3.84 for one degree of freedom (*df*) or by 5.99 for two *df* is associated with an α of 0.05 according to a chi-square distribution (likelihood ratio test)

[e] The release from nanodroplets during sample handling was assumed to be saturable due to the solubility of paclitaxel in plasma. The model predicted that a small fraction (on average about 1%) of unreleased paclitaxel in nanodroplets contributed to the observed concentration in plasma ultrafiltrate (see also Figs. 1, 5)

that is released directly into the DPC is Fr3. The remainder fraction of dose (1 − Fr3) is released simultaneously into the central compartment. Models with a direct release into the shallow peripheral compartment were also considered.

Observation model for Tocosol Paclitaxel

The following output equation was used to describe the total paclitaxel concentration (C_t) in whole blood for Tocosol Paclitaxel:

$$C_t = \frac{A_{Nano}}{V_{Nano}} + \frac{A1 \cdot BF_{TOC}}{V1} \quad (5)$$

$$BF_{TOC} = \left(1 + B_P + \frac{B_{Sat,P}}{K_d + C1}\right). \quad (6)$$

The binding factor (BF_{TOC}) for Tocosol Paclitaxel is the ratio of total blood to unbound plasma concentration and B_P describes the linear binding and $B_{Sat,P}$ (maximum binding capacity) and K_d (dissociation constant) the saturable binding of paclitaxel to proteins and blood cells. It was assumed that the volume of distribution for nanodroplets includes plasma and that elimination of nanodroplets during the release phase was negligible. We assumed that paclitaxel is released from drug-containing Tocosol nanodroplets during processing of blood samples and assumed such time averaged 30 min. This choice only affects the estimate for half-life of drug release during centrifugation. The output equation for the drug concentration in plasma ultrafiltrate is derived in Appendix for Tocosol Paclitaxel.

Input and disposition models for Taxol

The drug input for Taxol was specified as a time-delimited zero-order input of paclitaxel into the central paclitaxel compartment and of Cremophor into the (central) Cremophor compartment (Fig. 1). For Taxol, the same disposition models as for Tocosol Paclitaxel were considered and the linear model for disposition of unbound paclitaxel as shown above for Tocosol Paclitaxel except for the saturable release from Tocosol nanodroplets was used as the final model.

Disposition of Cremophor was assessed with one-, two-, or three-compartment models with first-order elimination. As Cremophor concentrations were not measured, the volume of distribution for Cremophor was fixed to a literature estimate [38] of 6.01 L. As Cremophor concentrations were not measured in this study, the choice of this volume only affects the estimate for the Cremophor clearance and the parameter(s) for binding of paclitaxel to Cremophor but no other model parameter. Additionally, we incorporated the model from van den Bongard et al. [38] to describe the disposition of Cremophor.

Observation model for Taxol

The following output equation was used to describe the total concentration of paclitaxel in whole blood based on the modeled Cremophor concentration (C_{CrEL}, equation for Cremophor disposition not shown):

$$C_t = \frac{A1 \cdot BF_{Taxol}}{V1} \quad (7)$$

$$BF_{Taxol} = \left(1 + B_P + \frac{B_{Sat,P}}{K_d + C1} + B_{CrEL} \cdot C_{CrEL}\right). \quad (8)$$

The binding factor for Taxol (BF_{Taxol}) contained one term describing the linear binding of paclitaxel to Cremophor (B_{CrEL}) in addition to the same terms as the binding factor for Tocosol Paclitaxel. It was assumed that the (central) volume of distribution for Cremophor includes the plasma volume. For Taxol, the paclitaxel concentration in plasma ultrafiltrate was the paclitaxel concentration in the central compartment.

Size model

The BSA was calculated by the Mosteller formula [24] and used to describe body size and to scale all clearance and volume terms linearly by BSA. The fractional change ($F_{Size,i}$) in clearance and volume of distribution for the ith subject (with BSA_i) standardized to a BSA_{STD} of 1.73 m^2 is: $F_{Size,i} = BSA_i/BSA_{STD}$.

Parameter variability model for PK

The between-subject variability (BSV) of PK parameters was estimated by assuming a log-normal distribution. The η_{BSVi} is the log scale difference of the individual PK parameter estimate from its population mean for the *i*th subject. It is assumed that η_{BSV} is a normally distributed random variable with mean zero and standard deviation BSV. The BSV was estimated as variance. We report the %CV of a normal distribution on log-scale calculated by the formula $\%CV = [\exp(\text{variance}) - 1]^{0.5}$. The individual PK parameters were calculated as $CL_i = CL_{POP} \cdot F_{Size,i} \cdot \exp(\eta_{BSVCL,i})$.

The CL_{POP} is the group estimate of clearance for a patient of standard body size (BSA_{STD}), CL_i is the individual clearance for the *i*th subject, and η_{BSVCLi} is the individual log-scale difference for clearance in the *i*th subject from the population mean. Similar formulas apply to the other PK parameters. Individual disposition parameter estimates were assumed to be the same for both formulations. Between-occasion variability of PK parameters was assumed to be small and was not included in the final model.

Residual unidentified variability

The residual unidentified variability was described by a combined additive and proportional error model for paclitaxel concentrations in plasma ultrafiltrate and whole blood.

Estimation

NONMEM® version VI level 1.1 (NONMEM Project Group, University of California, San Francisco, CA) [1] was used for population PK analysis. The first-order conditional estimation (FOCE) method with the interaction

estimation option in NONMEM was used for all analyses. Confidence intervals for model parameters were obtained by non-parametric bootstrapping with 35 randomly selected patients in each of the 500 bootstrap replicates.

Model qualification

The models were compared by their predictive performance, the objective function in NONMEM, individual model fits, observed versus predicted plots, and standard diagnostic plots. Predictive performance was assessed by visual predictive checks based on at least 6,000 virtual patients.

Monte Carlo simulations

Monte Carlo simulations were run in absence of residual error for 1,000 virtual patients to assess the paclitaxel release profile of Tocosol Paclitaxel and the disposition of Tocosol Paclitaxel and Taxol and calculate the median and 80% non-parametric prediction interval.

Non-compartmental analysis (NCA), statistics, and software

WinNonlin™ Professional (version 5.0.1, Pharsight Corp., Mountain View, CA) was used for NCA. The ANOVA and equivalence statistics with factors accounting for sequence, subject nested within sequence, period and treatment effects was obtained with SAS (version 9.1.3 for Windows, SAS Institute, Cary, NC). Maple© 10.05 (Maplesoft, Waterloo, ON, Canada) was used to explicitly solve the differential equations for the output equation.

Results

Patients

One patient dropped out after having received 48 mg Tocosol Paclitaxel during the first 2 min of the infusion. This patient was excluded from all PK analyses, as no post-dose blood samples were collected. The remaining 35 patients had heights of 167 ± 9.7 cm, total body weights of 68.5 ± 17.3 kg, BSA of 1.77 ± 0.23 m^2, and ages of 58.6 ± 12.5 years (mean ± SD). Six patients were African Americans (5 females/1 male) and 29 patients were Caucasians (15 females/14 males). The ECOG performance status was 0 for 4 patients, 1 for 19 patients, and 2 for 12 patients. Type of primary cancer was breast in 9 patients, gastrointestinal in 6 patients, head and neck in 5 patients, lung in 3 patients, and 'other' in 12 patients.

Of those 35 patients, 7 patients (2 patients for Taxol and 5 patients for Tocosol Paclitaxel) had their paclitaxel infusion interrupted and resumed within 30 min. Three patients (1 patient for Tocosol Paclitaxel and 2 patients for Taxol) dropped out before receiving the dose in study period II. As those patients contributed data from study period I, these three patients were included in the population PK analysis. However, these three patients and one patient with insufficient data for NCA in study period I were excluded from NCA and ANOVA statistics.

NCA

Figure 2 shows the median plasma concentrations for paclitaxel in plasma ultrafiltrate and in whole blood. Ultrafiltrate concentrations for Tocosol Paclitaxel revealed the prolonged release of paclitaxel from nanodroplets. Total concentrations showed a sharp peak at 0.25 h for Tocosol Paclitaxel. There was no apparent prolonged release for Taxol.

The following data are geometric means (%CV). Area under the curve from time zero to infinity was 603 ng h/mL (22%) for Tocosol Paclitaxel and 360 ng h/mL (23%) for Taxol in plasma ultrafiltrate and was 29.9 × 10^3 ng h/mL (27%) for Tocosol Paclitaxel and 14.3 × 10^3 ng h/mL (27%) for Taxol. Total clearance was 511 L/h (28%) for Tocosol Paclitaxel and 852 L/h (29%) for Taxol in plasma ultrafiltrate and was 10.3 L/h (33%) for Tocosol Paclitaxel and 21.4 L/h (32%) for Taxol in whole blood. Terminal half-life was 26.0 h (26%) for Tocosol Paclitaxel and 25.2 h (28%) for Taxol in plasma ultrafiltrate and was 21.5 h (26%) for Tocosol Paclitaxel and 22.9 h (37%) for Taxol in whole blood. The ratio of AUC for Tocosol Paclitaxel divided by Taxol was 1.67 (1.55–1.80) for ultrafiltrate concentrations and 2.08 (1.97–2.20) for whole blood concentrations [point estimate (90% confidence interval) from ANOVA].

Population PK model

Visual predictive checks and the log-likelihood significantly favored a three- versus two-compartment disposition model. After accounting for the time-dependent binding of paclitaxel to Cremophor due to elimination of Cremophor and for the unreleased drug in nanodroplets in blood samples, models with saturable elimination or saturable distribution neither improved the objective function nor the predictive performance compared to models with first-order disposition of unbound paclitaxel.

Linear and saturable binding to plasma proteins and red blood cells (combined) and linear and saturable binding to Cremophor were considered. The final model included linear and saturable binding to plasma proteins and red

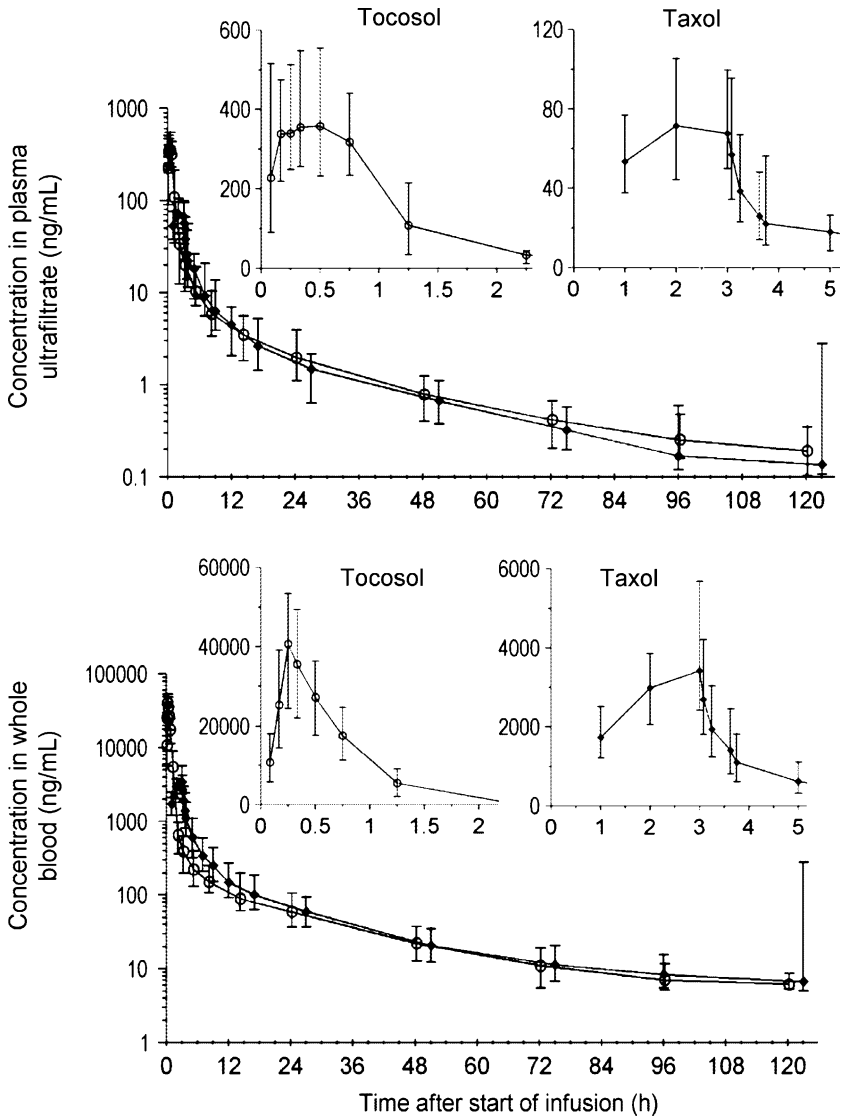

Fig. 2 Median (10–90% percentile) paclitaxel concentrations versus time after administration of Tocosol Paclitaxel (*left*, *open circles*) and Taxol (*right*, *filled diamonds*). *Inserts* show early time profiles

blood cells and linear binding to Cremophor (Fig. 1). Use of a one-compartment PK model for Cremophor significantly improved the model fits and log-likelihood compared to models with a constant Cremophor concentration. When multi-compartment models for Cremophor with first-order elimination were estimated, the objective function improved by 41 for the two-compartment Cremophor model and by 49 for the three-compartment Cremophor model both relative to the one-compartment model. However, the individual curve fits, the population predicted versus observed and individual predicted versus observed plots were very similar for one-, two- and three-compartment models for Cremophor. As we did not measure Cremophor concentrations, the one-compartment model was chosen following the rule of parsimony. Use of the population PK model for Cremophor from van den Bongard et al. [38] yielded a considerably worse objective function (increase by 118).

Drug input for Taxol was described adequately by zero-order input into the central compartment. For Tocosol Paclitaxel, a mixed-order release from the nanodroplet to the central compartment (Fig. 1) improved the predictive performance and the log-likelihood significantly compared to models with first-order release. The output equations accounted for drug entrapped in Cremophor micelles (Taxol only) and unreleased drug in nanodroplets (Tocosol Paclitaxel only). The volume of distribution of the nanodroplets was estimated to be 6.66 L (21% CV). The objective function improved significantly, when release of paclitaxel during sample handling was included (Fig. 1).

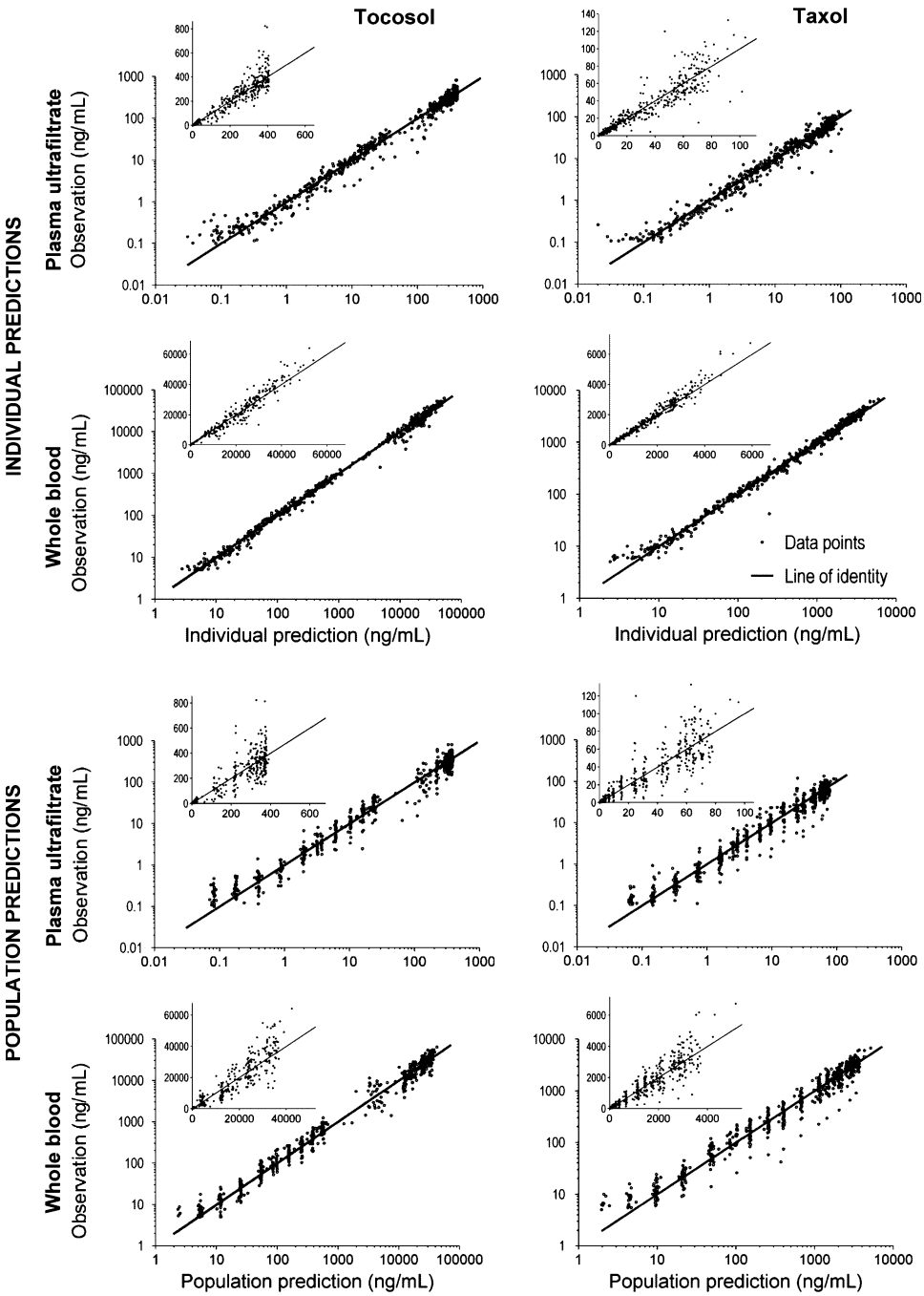

Fig. 3 Observations versus individual predictions (*top rows*) and observations versus population predictions (*bottom rows*) for paclitaxel concentrations in plasma ultrafiltrate and whole blood on logarithmic scale (*inserts* show the same data on linear scale). The assumed solubility limit of unbound paclitaxel that was estimated as 405 ng/mL causes the boundary in the *top left panel* (see Fig. 1; Table 1)

Without this feature, model fits were biased and models could not predict the complex time course for the ratio of concentrations in plasma ultrafiltrate and whole blood.

The final population PK parameter estimates are shown in Table 1. Plots of observed versus individual predicted concentrations (Fig. 3, top) indicated unbiased and precise fits for plasma ultrafiltrate and whole blood for both treatments. There was no bias for observed concentrations versus population predictions (Fig. 3, bottom). As these predicted versus observed plots indicated precise and unbiased fits without including between occasion variability in the model, between occasion variability was probably rather small and was not included in the final model. Visual predictive checks of the final population PK model revealed excellent predictive performance for Tocosol Paclitaxel and Taxol, as the central tendency and variability of the observed concentrations were well captured (Fig. 4). The model also captured the time course of the ratio of observed concentrations in plasma ultrafiltrate and whole blood.

Allowing a small amount of the dose to be released from nanodroplets into the DPC improved the objective function

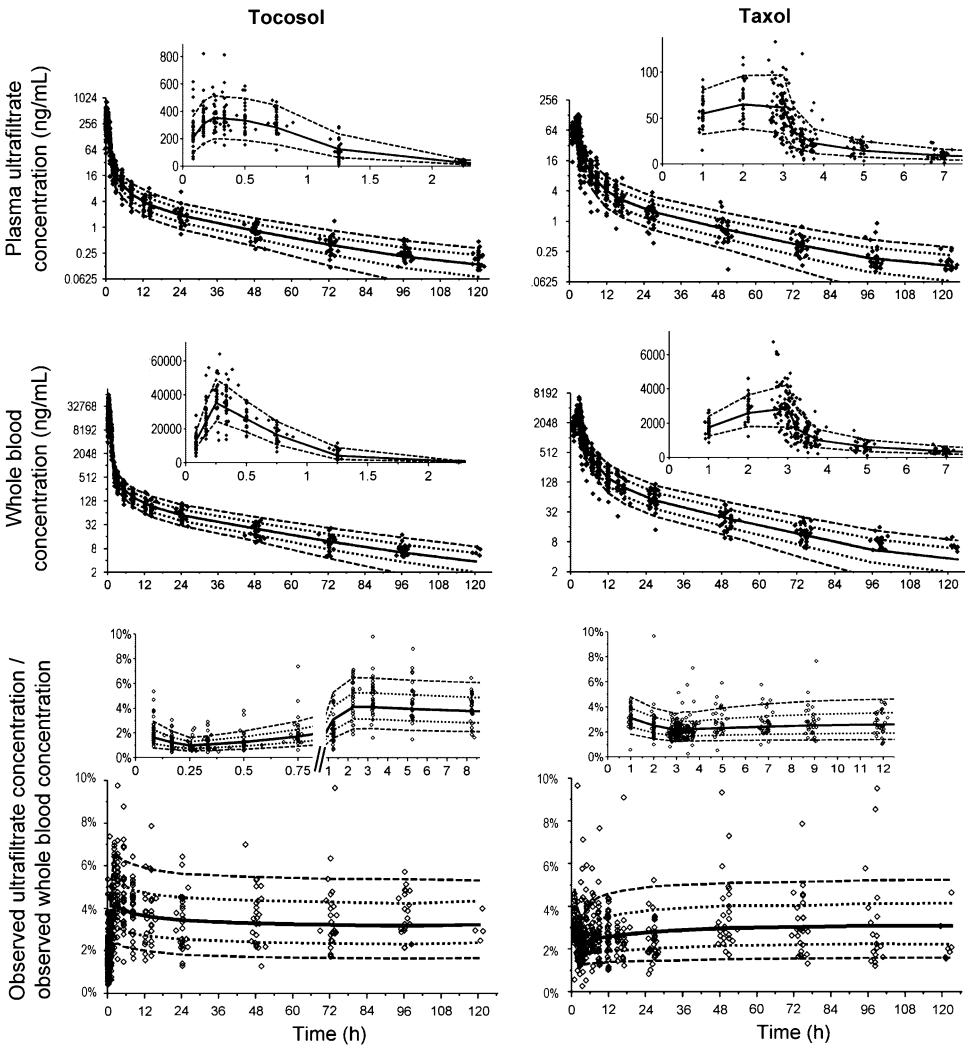

Fig. 4 Visual predictive check for paclitaxel concentrations in plasma ultrafiltrate and in whole blood based on 10,000 simulated, virtual patients. Data are median, 25–75% percentile (*dotted line*), and 10–90% percentile (*dashed line*). Ideally, 10% of the observations should fall outside the 10–90% percentile of simulated concentrations at each time point on each side

by 32.1 points ($P < 0.001$, likelihood ratio test). This fraction of dose was estimated to be 9.8%. Release from nanodroplets into the shallow peripheral compartment did not improve the objective function and the associated fraction of dose was estimated to be less than 1%. Therefore, direct release into the shallow peripheral compartment was not included in the final model.

The increase in the objective function after exclusion of one specific model component is shown in Table 1 with the final model as reference. After estimation of the simplified population PK models, the objective function favored the full model significantly ($P < 0.01$, likelihood ratio test) compared to each simplified model.

Monte Carlo simulations for a 15 min infusion of 300 mg Tocosol Paclitaxel showed that 90% of the dose was released into the central compartment or DPC after 1.14 ± 0.16 h (average $\pm$ SD). The prolonged release profile for Tocosol Paclitaxel nanodroplets is shown in Fig. 5a. During the first hour, the amount of drug in nanodroplets was the major fraction of the observed concentration in whole blood (Fig. 5b). These results were qualitatively consistent with an equilibrium dialysis study that showed a significantly slower in vitro release of paclitaxel for Tocosol Paclitaxel compared to Taxol (data on file at Sonus). The release from nanodroplets during sample handling was assumed to be saturable due to the solubility of paclitaxel in plasma. The model predicted that a small fraction (on average about 1%) of unreleased paclitaxel in nanodroplets contributed to the observed concentration in plasma ultrafiltrate. This small fraction causes plasma ultrafiltrate concentrations to be greater than unbound plasma concentrations during the first hour (Fig. 5c).

We simulated the unbound plasma concentrations which differ from ultrafiltrate concentrations in that unbound concentrations do not contain any drug released from nanodroplets during sample processing. A comparison of unbound plasma concentrations for Tocosol Paclitaxel and Taxol is shown in Fig. 5 for unbound concentrations in the

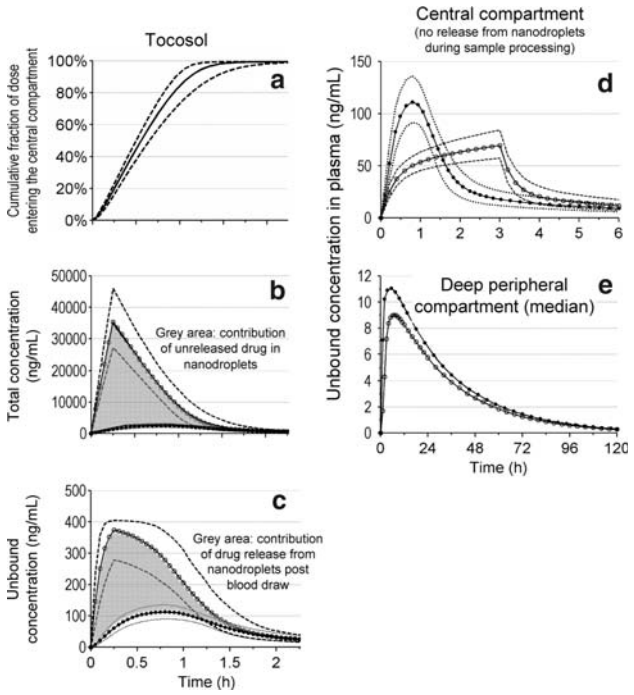

Fig. 5 Median (10–90% percentile) from 1,000 simulated patients with 1.73 m^2 BSA for a dose of 300 mg paclitaxel given as 15 min infusion (*Tocosol Paclitaxel*) or as 3 h infusion (*Taxol*) in absence of residual error; **a** cumulative fraction of dose reaching the central compartment, **b** observed total concentration (*open circle*) and total concentration without paclitaxel in nanodroplets (*filled circle*), **c** unbound concentration in plasma ultrafiltrate (*open circle*) and unbound plasma concentration without contribution from nanodroplets (*filled circle*), **d** and **e** unbound plasma concentration in central and deep peripheral compartment without release from nanodroplets sample processing (*Tocosol Paclitaxel*: *filled circle*, *Taxol*: *open circle*)

central compartment (d) and unbound concentrations in the DPC (e). Despite the substantially shorter duration of infusion (15 min for Tocosol Paclitaxel vs. 3 h for Taxol), the peak of the unbound concentrations was only about 60% higher for Tocosol Paclitaxel than for Taxol (Fig. 5d). The relative paclitaxel exposure in the central compartment for Tocosol Paclitaxel versus Taxol was 94% with a 90% confidence interval from 88 to 100%.

Discussion

A mechanistic population PK model is proposed that describes the release and disposition of paclitaxel in plasma ultrafiltrate and whole blood for a new tocopherol-based, Cremophor-free paclitaxel formulation and for Taxol. The model described simultaneously the release and disposition of unbound paclitaxel in plasma and binding to Cremophor, proteins, and red blood cells. The kinetics of nanodroplets and disposition of Cremophor were incorporated (Fig. 1). The final model had excellent predictive performance for paclitaxel concentrations in whole blood and plasma ultrafiltrate (Fig. 4) and could predict the complex time course of the ratio of plasma ultrafiltrate to whole blood concentrations. The low plasma ultrafiltrate to whole blood concentration ratios of about 1–2% from 0 to 1 h for Tocosol Paclitaxel (Fig. 4, bottom left panel) were consistent with the assumption that blood samples contained unreleased paclitaxel in nanodroplets (Fig. 5b).

Accounting for the release of paclitaxel during sample processing removed a systematic bias in the model fits and improved the objective function and predictive performance significantly. Although nanodroplets are stable for several hours in plasma (data on file at Sonus Pharmaceuticals), centrifugation to separate plasma from blood cells or ultrafiltration may release a small fraction of drug from the nanodroplets. The model predicted that on average only about 1% of the total unreleased paclitaxel in nanodroplets contributed to the observed concentration in plasma ultrafiltrate. As Cremophor is considered a high-affinity "binding site" for paclitaxel and as Cremophor micelles persist for several hours after dilution to concentrations below the critical micelle concentration of 0.009% (w/v, at equilibrium) [21, 34], no net release of paclitaxel from Cremophor micelles following blood sample collection was assumed.

The point estimates (90% confidence intervals) from NCA and ANOVA for the relative extent of bioavailability were 1.67 (1.55–1.80) for paclitaxel in plasma ultrafiltrate and 2.08 (1.97–2.20) for paclitaxel in whole blood for Tocosol Paclitaxel compared to Taxol. The PK model accounted for the time-course of drug release from nanodroplets and for the presence of drug-containing nanodroplets in blood samples (Figs. 1, 5b, c). As these processes cannot be accounted for by standard non-compartmental techniques, the NCA seems likely to provide biased estimates for drug exposure of slow release formulations given intravenously. In these cases, a modeling approach seems more appropriate. The estimated relative extent of bioavailability in the central compartment (90% confidence interval) from population PK modeling was 94% (88–100%). This estimate seems reasonable from a modeling perspective for two formulations administered intravenously. However, this estimate probably does not reflect the bioavailability at the site of toxicity (see companion article).

An alternative reason for a higher AUC for unbound paclitaxel would be a saturation of clearance at high concentrations. Earlier studies [11, 18–20, 30] presumed non-linearity in PK of total paclitaxel concentrations by saturable elimination and saturable distribution. More recent studies [9, 14–16, 32, 34] explained the apparent non-linearity of total paclitaxel by an entrapment of paclitaxel within Cremophor micelles with Cremophor concentrations

changing over time and dependent on Cremophor dose. Several studies [9, 14–16] successfully described the PK of unbound paclitaxel by linear two- or three-compartment models. A short (15 min) Tocosol Paclitaxel infusion yielded linear paclitaxel elimination and linear distribution for observed concentrations in plasma ultrafiltrate up to about 500 ng/mL. Human liver microsome data for CYP2C8 metabolism showed a high average Michaelis–Menten constant of 9 μM (equivalent to 7.7×10^3 ng/mL) [15]. Linear elimination was also found for docetaxel formulated with polysorbate 80 that is degraded rapidly in plasma [39]. These studies support first-order elimination of paclitaxel.

Our estimated terminal half-life of unbound paclitaxel was in good agreement with the terminal half-life from Henningsson et al. [15] who used a comparable sampling schedule. The estimate for total clearance of paclitaxel in whole blood (Table 1) was within the reported range of clearances for total paclitaxel [7, 13, 17, 25]. Our unbound clearance of 845 L/h (25% CV for BSV) was higher than the range of average unbound clearances from 301 to 429 L/h in the literature [9, 14–16]. The BSV in unbound clearance was up to 44% with individual clearances ranging from 83.7 to 1,055 L/h [15]. Literature studies [9, 14–16] applied equilibrium dialysis with a tritiated paclitaxel tracer [3] to determine unbound concentrations, whereas paclitaxel in plasma ultrafiltrate was determined by LC–MS/MS in this study. This could have contributed to the differences in clearance of unbound paclitaxel. Further studies are required to resolve these differences.

As we did not measure Cremophor, the volume of distribution of Cremophor was fixed to the estimate from van den Bongard et al. [38]. Our estimate for Cremophor clearance of 0.583 L/h was at the upper end of the range of Cremophor clearances in literature [9, 10, 35, 41], if areas up to the last quantifiable concentration were used for clearance calculation. The median of the individual Cremophor half-lives was 10.6 h in this study. This half-life was estimated from binding of paclitaxel to Cremophor that changes over time due to elimination of Cremophor. Cremophor is a non-ionic surfactant consisting of a complex mixture of chemical compounds [31]. Therefore, this half-life reflects the net half-life of the Cremophor component(s) relevant for paclitaxel binding. Terminal half-lives up to about 100 h were reported for Cremophor [10, 35]. We found longer terminal half-lives, when we tested two- and three-compartment models for Cremophor. As these models did not improve any critical feature of the model and provided essentially indistinguishable curve fits, the simplest one-compartment model for Cremophor was chosen as the final model. Cremophor binding was probably less important at lower Cremophor concentrations that might have dropped below the critical micelle concentration for Cremophor [21].

We posited saturable paclitaxel release from nanodroplets into blood and saturable release of paclitaxel during sample processing based on the low aqueous solubility of paclitaxel. The estimate for paclitaxel solubility of 405 ng/mL (equivalent to 0.47 μM) for unbound paclitaxel in plasma is in good agreement with the observed paclitaxel solubility of 0.4 μM (range: 0.2–0.9 μM) at equilibrium [12, 29, 37]. It was encouraging to see that implementing a physicochemical mechanism improved the objective function, model fits, and predictive performance significantly. Figure 2 shows a "plateau" of concentrations in plasma ultrafiltrate for Tocosol Paclitaxel, whereas the associated concentrations in whole blood showed a pronounced peak. Saturable binding of paclitaxel would cause the opposite behavior. The final model predicted the time course of plasma ultrafiltrate and whole blood concentrations as well as their ratio (Fig. 4). In agreement with results of a phase I dose escalation study with Tocosol Paclitaxel [36], the model predicted a slightly more than proportional increase of whole blood AUC with dose. In addition, the model predicted an approximately proportional increase of plasma ultrafiltrate AUC and a proportional increase of unbound paclitaxel AUC in the central compartment for Tocosol Paclitaxel doses from 25 to 225 mg/m^2.

Prolonged release of paclitaxel from nanodroplets was found (Fig. 5a) that supports administering Tocosol Paclitaxel as a 15 min infusion. Additionally, the new Cremophor-free Tocosol Paclitaxel formulation does not carry the risk for Cremophor-related toxicity. A small fraction (9.8%) of Tocosol Paclitaxel dose was estimated to enter directly into the DPC. As models with a direct release of paclitaxel into the shallow peripheral compartment did not improve the objective function and as the associated fraction of dose was minimal (<1%), only release into the deep peripheral compartment was included in the final model. A direct release of a fraction of dose into the deep peripheral compartment increases the unbound AUC in this compartment much more compared to a direct release of the same fraction of dose into the shallow peripheral compartment, since the equilibration between the shallow peripheral and central compartment was much faster than the equilibration for the deep peripheral compartment. As described in the companion article, the direct release of drug into the deep peripheral compartment was one mechanism that explained differences in toxicity.

As Tocosol Paclitaxel nanodroplets have a diameter of 40–80 nm [5, 6] and as pore sizes of many tumor tissues are larger than tight endothelial junctions of normal tissue vasculature [28], this estimate seems reasonable (see companion article for a more detailed discussion). Nanodroplets were assumed to release a small fraction (9.8%) of the Tocosol Paclitaxel dose into the whole DPC (Fig. 5e). If only a part of the DPC is accessible to nanodroplet release,

paclitaxel concentrations at these sites will have greater unbound concentrations than shown in Fig. 5e. Tocosol Paclitaxel might therefore show more toxicity at sites accessible to release from nanodroplets compared to Taxol at the same dose. More toxicity for Tocosol Paclitaxel has been observed for neutrophil counts (see companion article).

In conclusion, the proposed mechanistic population PK model showed that disposition of unbound paclitaxel was linear. The prolonged release of paclitaxel from Tocosol Paclitaxel nanodroplets was well described by a solubility-limited process. For a 15 min Tocosol Paclitaxel intravenous infusion, the average (±SD) time to 90% cumulative drug input was predicted to be 1.14 ± 0.16 h. Predicted unbound peak paclitaxel plasma concentrations were about 60% (median) higher for a 15 min Tocosol Paclitaxel infusion compared to a 3 h Taxol infusion, due to the prolonged release for Tocosol Paclitaxel and limited solubility of paclitaxel. The prolonged paclitaxel release supports 15 min infusion of Tocosol Paclitaxel. A small fraction of dose (9.8%) was estimated to be directly released into the DPC. The PK model proposed herein that is predicated on the limited solubility of paclitaxel may be important to optimize dosage regimens for nanodroplet formulations of drugs with a low aqueous solubility like paclitaxel.

Acknowledgments We thank Dr. Louis Goedhals, Dr. Young Lee, and Dr. Jan Vermorken for leading the clinical study at their study site. This study was supported by Sonus Pharmaceuticals, Inc. This clinical study was performed by Sonus Pharmaceuticals, Inc., and the modeling was supported by Sonus Pharmaceuticals. Jürgen Bulitta was supported by a post-doctoral fellowship from Johnson & Johnson.

Conflicts of interest statement The work presented in this manuscript was supported by Sonus Pharmaceuticals, Inc.

Appendix

Mechanistic model for drug release from Tocosol Paclitaxel nanodroplets

The following equations describe the amount of paclitaxel in nanodroplets (A_{Nano}) and in the unstirred water layer (A_{Layer}) (see also Fig. 1):

$$\frac{dA_{Nano}}{dt} = F_{Tocosol} \cdot R_{Input} - ka_1 \cdot \left(1 - \frac{C_{Layer}}{C_{Sol}}\right) \cdot A_{Nano} \quad (A1)$$

$$\frac{dA_{Layer}}{dt} = ka_1 \cdot \left(1 - \frac{C_{Layer}}{C_{Sol}}\right) \cdot A_{Nano} - ka_2 \cdot A_{Layer} \quad (A2)$$

where C_{Sol} is the solubility of unbound paclitaxel in the volume of distribution for nanodroplets (V_{Nano}), C_{Layer} is the paclitaxel concentration in the unstirred water layer, R_{Input} is the zero-order input into the nanodroplet compartment, and $F_{Tocosol}$ is the relative bioavailability of Tocosol Paclitaxel compared to Taxol. The release of drug from nanodroplets into the unstirred water layer is described by the first-order rate constant ka_1 and the transfer of drug from the unstirred water layer to the central and peripheral compartment by the first-order rate constant ka_2 (Fig. 1). Initial conditions for A_{Nano} and A_{Layer} are zero.

If ka_2 is much larger than ka_1, A_{Layer} will show a rapid initial rise and thereafter the differential dA_{Layer}/dt will be very small compared to dA_{Nano}/dt. In this situation, the quasi-stationary solution for A_{Layer} that is valid after the rapid initial rise can be calculated by setting the differential dA_{Layer}/dt to zero and solving for A_{Layer}. This yields:

$$A_{Layer} = \frac{ka_1 \cdot A_{Nano}}{ka_2 + \frac{ka_1 \cdot A_{Nano}}{C_{Sol} \cdot V_{Layer}}}. \quad (A3)$$

The V_{Layer} represents the volume of the unstirred water layer. Inserting this equation into Eq. A1 yields the following equation for the mixed-order (Michaelis–Menten) process from the nanodroplet to the central compartment:

$$\begin{aligned}\frac{dA_{Nano}}{dt} &= F_{Tocosol} \cdot R_{Input} - \frac{ka_2 \cdot C_{Sol} \cdot V_{Layer} \cdot A_{Nano}}{\frac{ka_2 \cdot C_{Sol} \cdot V_{Layer}}{ka_1} + A_{Nano}} \\ &= F_{Tocosol} \cdot R_{Input} - \frac{Vmax \cdot A_{Nano}}{AN_{50} + A_{Nano}}. \end{aligned} \quad (A4)$$

The maximum rate of drug transfer is denoted as V_{max} and is equal to the product of ka_2, C_{Sol}, and V_{Layer}. The amount of drug in the nanodroplet compartment (AN_{50}) that results in a transfer rate of 50% of V_{max} is V_{max}/ka_1. Based on the final estimates, we confirmed that this quasi-stationary solution is an accurate approximation of the full set of differential equations.

The product of ka_2 and V_{Layer} is the clearance from the unstirred water layer (CL_{Layer}) which is identifiable, whereas the individual terms are not. Therefore, a mixed-order transfer from the nanodroplet to the central compartment can be explained mechanistically by solubility-limited transfer through an unstirred water layer.

Output equation for plasma ultrafiltrate for nanodroplet formulation

Blood samples drawn during the release phase of Tocosol Paclitaxel nanodroplets contain nanodroplets with paclitaxel. This unreleased paclitaxel was assumed to be in part released during the processing of blood samples. Due to the

vigorous conditions during centrifugation, we assumed that the unstirred water layer is less important. The release of paclitaxel from nanodroplets into plasma was described by a first-order process that becomes saturated, if the unbound plasma concentration approaches the estimated solubility limit (Fig. 1). This yields the following equations for the amounts of drug in nanodroplets in a blood sample ($A_{Nano,S}$) and in the blood sample excluding drug in nanodroplets ($A_{Blood,S}$):

$$\frac{dA_{Nano,S}}{dt} = -ka \cdot A_{Nano,S} \cdot \left(1 - \frac{A_{Blood,S}}{V_{Sample} \cdot BF_{TOC} \cdot C_{Sol}}\right) \quad (A5)$$

$$\frac{dA_{Blood,S}}{dt} = ka \cdot A_{Nano,S} \cdot \left(1 - \frac{A_{Blood,S}}{V_{Sample} \cdot BF_{TOC} \cdot C_{Sol}}\right). \quad (A6)$$

The binding factor for Tocosol paclitaxel (BF_{TOC}) was assumed to be constant during sample handling, as the saturable component of protein binding was negligible for high unbound concentrations. The first-order release rate constant under sample handling conditions is denoted as ka. The paclitaxel amount in sampled blood excluding drug in nanodroplets ($A_{Blood,S}$) divided by the sample volume (V_{Sample}) and by the binding factor BF_{TOC} yields the unbound plasma concentration. The initial condition was $A_{Nano} \cdot V_{Sample}/V_{Nano}$ for $A_{Nano,S}$ and the unbound concentration in central compartment (C1) multiplied by V_{Sample} and BF_{TOC} for $A_{Blood,S}$.

These two differential equations were solved in Maple and the solution was used as the output equation for the paclitaxel concentration in plasma ultrafiltrate for Tocosol Paclitaxel [$E(t_{Proc})$, N1, and N2 are intermediary variables to simplify the equations]:

$$E(t_{Proc}) = \exp\left(\frac{ka \cdot (A_{Nano} - V_{Nano} \cdot C_{Sol} \cdot BF_{TOC} + V_{Nano} \cdot BF_{TOC} \cdot C1) \cdot t_{Proc}}{V_{Nano} \cdot BF_{TOC} \cdot C_{Sol}}\right) \quad (A7)$$

$$N1 = -C_{Sol} \cdot A_{Nano} + A_{Nano} \cdot C1 - V_{Nano} \cdot C_{Sol} \cdot BF_{TOC} \cdot C1 \quad (A8)$$

$$N2 = V_{Nano} \cdot BF_{TOC} \cdot C1^2 + C_{Sol} \cdot E(t_{Proc}) \cdot A_{Nano} \quad (A9)$$

$$A_{blood,S}(t_{Proc}) = \frac{V_{Sample} \cdot BF_{TOC} \cdot [N1 + N2]}{-BF_{TOC} \cdot C_{Sol} \cdot V_{Nano} + V_{Nano} \cdot BF_{TOC} \cdot C1 + E(t_{Proc}) \cdot A_{Nano}}. \quad (A10)$$

Dividing the amount of paclitaxel in the blood sample (excluding the unreleased amount in nanodroplets) at the end of sample processing (t_{Proc}) by the sample volume and the binding factor yields the output equation for the concentration in plasma ultrafiltrate for Tocosol Paclitaxel:

$$Cu(t_{Proc}) = \frac{A_{blood,S}(t_{Proc})}{V_{Sample} \cdot BF_{TOC}}. \quad (A11)$$

We assumed an average time of sample processing of 30 min according to the procedures described in the clinical protocol and estimated the half-life of the first-order release rate constant ka. The sample volume (V_{Sample}) was arbitrarily set to 1 L, as this choice did not influence the results.

References

1. Beal SL, Sheiner LB, Boeckmann AJ (2006) NONMEM Users Guides (1989–2006). Icon Development Solutions, Ellicott City
2. Brat DJ, Windebank AJ, Brimijoin S (1992) Emulsifier for intravenous cyclosporin inhibits neurite outgrowth, causes deficits in rapid axonal transport and leads to structural abnormalities in differentiating N1E.115 neuroblastoma. J Pharmacol Exp Ther 261:803–810
3. Brouwer E, Verweij J, De Bruijn P, Loos WJ, Pillay M, Buijs D, Sparreboom A (2000) Measurement of fraction unbound paclitaxel in human plasma. Drug Metab Dispos 28:1141–1145
4. Brown T, Havlin K, Weiss G, Cagnola J, Koeller J, Kuhn J, Rizzo J, Craig J, Phillips J, Von Hoff D (1991) A phase I trial of taxol given by a 6-hour intravenous infusion. J Clin Oncol 9:1261–1267
5. Constantinides PP, Lambert KJ, Tustian AK, Schneider B, Lalji S, Ma W, Wentzel B, Kessler D, Worah D, Quay SC (2000) Formulation development and antitumor activity of a filter-sterilizable emulsion of paclitaxel. Pharm Res 17:175–182
6. Constantinides PP, Tustian A, Kessler DR (2004) Tocol emulsions for drug solubilization and parenteral delivery. Adv Drug Deliv Rev 56:1243–1255
7. Dhanikula AB, Panchagnula R, Singh I, Kaur KJ, Kaul CL, Sekhon JS (2001) Pharmacokinetic study of paclitaxel as a 3-hour infusion in an Indian population: 135 mg/m2 vs. 175 mg/m2. Methods Find Exp Clin Pharmacol 23:93–98
8. Dorr RT (1994) Pharmacology and toxicology of Cremophor EL diluent. Ann Pharmacother 28:S11–S14
9. Gelderblom H, Mross K, ten Tije AJ, Behringer D, Mielke S, van Zomeren DM, Verweij J, Sparreboom A (2002) Comparative pharmacokinetics of unbound paclitaxel during 1- and 3-hour infusions. J Clin Oncol 20:574–581
10. Gelderblom H, Verweij J, Brouwer E, Pillay M, de Bruijn P, Nooter K, Stoter G, Sparreboom A (1999) Disposition of [G-(3)H]paclitaxel and cremophor EL in a patient with severely impaired renal function. Drug Metab Dispos 27:1300–1305
11. Gianni L, Kearns CM, Giani A, Capri G, Vigano L, Lacatelli A, Bonadonna G, Egorin MJ (1995) Nonlinear pharmacokinetics and metabolism of paclitaxel and its pharmacokinetic/pharmacodynamic relationships in humans. J Clin Oncol 13:180–190
12. Hamada H, Ishihara K, Masuoka N, Mikuni K, Nakajima N (2006) Enhancement of water-solubility and bioactivity of paclitaxel using modified cyclodextrins. J Biosci Bioeng 102:369–371
13. Hempel G, Rube C, Mosler C, Wienstroer M, Wagner-Bohn A, Schuck A, Willich N, Boos J (2003) Population pharmacokinetics of low-dose paclitaxel in patients with brain tumors. Anticancer Drugs 14:417–422

14. Henningsson A, Karlsson MO, Vigano L, Gianni L, Verweij J, Sparreboom A (2001) Mechanism-based pharmacokinetic model for paclitaxel. J Clin Oncol 19:4065–4073
15. Henningsson A, Marsh S, Loos WJ, Karlsson MO, Garsa A, Mross K, Mielke S, Vigano L, Locatelli A, Verweij J, Sparreboom A, McLeod HL (2005) Association of CYP2C8, CYP3A4, CYP3A5, and ABCB1 polymorphisms with the pharmacokinetics of paclitaxel. Clin Cancer Res 11:8097–8104
16. Henningsson A, Sparreboom A, Sandstrom M, Freijs A, Larsson R, Bergh J, Nygren P, Karlsson MO (2003) Population pharmacokinetic modelling of unbound and total plasma concentrations of paclitaxel in cancer patients. Eur J Cancer 39:1105–1114
17. Ibrahim NK, Desai N, Legha S, Soon-Shiong P, Theriault RL, Rivera E, Esmaeli B, Ring SE, Bedikian A, Hortobagyi GN, Ellerhorst JA (2002) Phase I and pharmacokinetic study of ABI-007, a Cremophor-free, protein-stabilized, nanoparticle formulation of paclitaxel. Clin Cancer Res 8:1038–1044
18. Joerger M, Huitema AD, van den Bongard DH, Schellens JH, Beijnen JH (2006) Quantitative effect of gender, age, liver function, and body size on the population pharmacokinetics of Paclitaxel in patients with solid tumors. Clin Cancer Res 12:2150–2157
19. Karlsson MO, Molnar V, Freijs A, Nygren P, Bergh J, Larsson R (1999) Pharmacokinetic models for the saturable distribution of paclitaxel. Drug Metab Dispos 27:1220–1223
20. Kearns CM, Gianni L, Egorin MJ (1995) Paclitaxel pharmacokinetics and pharmacodynamics. Semin Oncol 22:16–23
21. Kessel D (1992) Properties of cremophor EL micelles probed by fluorescence. Photochem Photobiol 56:447–451
22. Kumar GN, Walle UK, Bhalla KN, Walle T (1993) Binding of taxol to human plasma, albumin and alpha 1-acid glycoprotein. Res Commun Chem Pathol Pharmacol 80:337–344
23. Monsarrat B, Alvinerie P, Wright M, Dubois J, Gueritte-Voegelein F, Guenard D, Donehower RC, Rowinsky EK (1993) Hepatic metabolism and biliary excretion of Taxol in rats and humans. J Natl Cancer Inst Monogr 15:39–46
24. Mosteller RD (1987) Simplified calculation of body-surface area. N Engl J Med 317:1098
25. Mould DR, Fleming GF, Darcy KM, Spriggs D (2006) Population analysis of a 24-h paclitaxel infusion in advanced endometrial cancer: a gynaecological oncology group study. Br J Clin Pharmacol 62:56–70
26. Oken MM, Creech RH, Tormey DC, Horton J, Davis TE, McFadden ET, Carbone PP (1982) Toxicity and response criteria of the Eastern Cooperative Oncology Group. Am J Clin Oncol 5:649–655
27. Rowinsky EK, Eisenhauer EA, Chaudhry V, Arbuck SG, Donehower RC (1993) Clinical toxicities encountered with paclitaxel (Taxol). Semin Oncol 20:1–15
28. Sapra P, Tyagi P, Allen TM (2005) Ligand-targeted liposomes for cancer treatment. Curr Drug Deliv 2:369–381
29. Sharma US, Balasubramanian SV, Straubinger RM (1995) Pharmaceutical and physical properties of paclitaxel (Taxol) complexes with cyclodextrins. J Pharm Sci 84:1223–1230
30. Sonnichsen DS, Hurwitz CA, Pratt CB, Shuster JJ, Relling MV (1994) Saturable pharmacokinetics and paclitaxel pharmacodynamics in children with solid tumors. J Clin Oncol 12:532–538
31. Sparreboom A, Loos WJ, Verweij J, de Vos AI, van der Burg ME, Stoter G, Nooter K (1998) Quantitation of Cremophor EL in human plasma samples using a colorimetric dye-binding microassay. Anal Biochem 255:171–175
32. Sparreboom A, van Tellingen O, Nooijen WJ, Beijnen JH (1996) Nonlinear pharmacokinetics of paclitaxel in mice results from the pharmaceutical vehicle Cremophor EL. Cancer Res 56:2112–2115
33. Sparreboom A, van Tellingen O, Nooijen WJ, Beijnen JH (1996) Tissue distribution, metabolism and excretion of paclitaxel in mice. Anticancer Drugs 7:78–86
34. Sparreboom A, van Zuylen L, Brouwer E, Loos WJ, de Bruijn P, Gelderblom H, Pillay M, Nooter K, Stoter G, Verweij J (1999) Cremophor EL-mediated alteration of paclitaxel distribution in human blood: clinical pharmacokinetic implications. Cancer Res 59:1454–1457
35. Sparreboom A, Verweij J, van der Burg ME, Loos WJ, Brouwer E, Vigano L, Locatelli A, de Vos AI, Nooter K, Stoter G, Gianni L (1998) Disposition of Cremophor EL in humans limits the potential for modulation of the multidrug resistance phenotype in vivo. Clin Cancer Res 4:1937–1942
36. Spigel SC, Jones SF, Greco FA (2002) S-8184 vitamin E paclitaxel emulsion: preclinical and phase 1 data. Proc Am Soc Clin Oncol 21. Abstract no. 406
37. Straubinger RM, Balasubramanian SV (2005) Preparation and characterization of taxane-containing liposomes. Methods Enzymol 391:97–117
38. van den Bongard HJ, Mathot RA, van Tellingen O, Schellens JH, Beijnen JH (2002) A population analysis of the pharmacokinetics of Cremophor EL using nonlinear mixed-effect modelling. Cancer Chemother Pharmacol 50:16–24
39. van Tellingen O, Beijnen JH, Verweij J, Scherrenburg EJ, Nooijen WJ, Sparreboom A (1999) Rapid esterase-sensitive breakdown of polysorbate 80 and its impact on the plasma pharmacokinetics of docetaxel and metabolites in mice. Clin Cancer Res 5:2918–2924
40. van Tellingen O, Huizing MT, Panday VR, Schellens JH, Nooijen WJ, Beijnen JH (1999) Cremophor EL causes (pseudo-) nonlinear pharmacokinetics of paclitaxel in patients. Br J Cancer 81:330–335
41. van Zuylen L, Karlsson MO, Verweij J, Brouwer E, de Bruijn P, Nooter K, Stoter G, Sparreboom A (2001) Pharmacokinetic modeling of paclitaxel encapsulation in Cremophor EL micelles. Cancer Chemother Pharmacol 47:309–318
42. van Zuylen L, Verweij J, Sparreboom A (2001) Role of formulation vehicles in taxane pharmacology. Invest New Drugs 19:125–141
43. Walle T, Walle UK, Kumar GN, Bhalla KN (1995) Taxol metabolism and disposition in cancer patients. Drug Metab Dispos 23:506–512
44. Weiss RB, Donehower RC, Wiernik PH, Ohnuma T, Gralla RJ, Trump DL, Baker JR Jr, Van Echo DA, Von Hoff DD, Leyland-Jones B (1990) Hypersensitivity reactions from taxol. J Clin Oncol 8:1263–1268
45. Wiernik PH, Schwartz EL, Einzig A, Strauman JJ, Lipton RB, Dutcher JP (1987) Phase I trial of taxol given as a 24-hour infusion every 21 days: responses observed in metastatic melanoma. J Clin Oncol 5:1232–1239
46. Wild MD, Walle UK, Walle T (1995) Extensive and saturable accumulation of paclitaxel by the human platelet. Cancer Chemother Pharmacol 36:41–44
47. Windebank AJ, Blexrud MD, de Groen PC (1994) Potential neurotoxicity of the solvent vehicle for cyclosporine. J Pharmacol Exp Ther 268:1051–1056